

# Synthesis of New Symmetrically Substituted Stilbenes with Large Multi-Photon Absorption Cross Section and Strong Two-Photon-Induced Blue Fluorescence

Xiaomei Wang, Guanyong Zhou, Dong Wang, Chun Wang, Qi Fang, and Minhua Jiang\*

State Key Laboratory of Crystal Materials, Shandong University Jinan, 250100, China

(Received January 15, 2001)

Efficient Ti-catalyzed reductive coupling methodology was first employed to synthesize three new chromophores, whose chemical structures have been characterized by IR,  $^1\text{H}$  NMR, MS spectra, and elemental analyses. These dye solutions exhibit the linear transmission of ca. 90% at wavelengths  $\geq 500$  nm at the concentrations of 0.005–0.0005 mol  $\text{dm}^{-3}$ . Pumped by ca. 700 nm laser irradiation, they possess large two-photon absorption cross sections of  $44.5 \times 10^{-48}$ – $62.0 \times 10^{-48}$   $\text{cm}^4 \text{ s photon}^{-1}$ , and strong up-conversion blue fluorescence occurring at 437–452 nm. A large three-photon absorption cross section of  $27.3 \times 10^{-76}$   $\text{cm}^6 \text{ s}^2 \text{ photon}^{-1}$  has also observed for one of these dyes under ca. 990 nm laser irradiation.

Two-photon absorption (2PA) is a subject which attracts fast-growing interest in the chemistry, photonics, and biological imaging communities recently. The 2PA process considering here involves the simultaneous absorption of two photons, either degenerating or nondegenerating, at wavelengths well beyond the linear absorption (1PA) spectrum of a particular molecule. This concept of the simultaneous absorption of two quanta of energy, predicted theoretically in 1931<sup>1</sup> and observed experimentally in the 1960s,<sup>2</sup> has now received much more consideration for the potentially practical applications such as optical power limiting, 3-D data storage, 3-D microfabrication and 3-D confocal microscopy and diagnostic/clinical therapy.<sup>3–6</sup> Multiphoton microscopy appears to have much greater value as an imaging technique for numerous biological applications as well as for nondestructive evaluation of organic paints and coatings.<sup>7–8</sup> The major feature<sup>9</sup> distinguishing one-photon absorption (1PA) from two-photon absorption (2PA) is the fact that the rate of energy (light) absorption is as a function of incident intensity. In one-photon absorption, the rate of light absorption is directly proportional to the incident intensity. By contrast, in simultaneous two-photon absorption, the rate of energy absorption is proportional to the square of the incident intensity. This quadratic or nonlinear dependence has substantial implications. For example, in a medium containing one-photon absorbing chromophores, significant absorption occurs all along the path of a focused light beam of suitable wavelength. This can lead to, e.g. photodegradation or photobleaching. In 2PA, negligible absorption occurs except in the immediate vicinity of the focal point of a light beam of appropriate energy. This allows spatial resolution along the beam axis and is the principal basis for two-photon fluorescence imaging.<sup>3</sup> The simultaneous absorption of two or more photons requires high peak power, which is now available from commercial ultrafast pulsed lasers. Thus, certain materials can undergo two-photon absorption at wavelengths far beyond

their linear absorption spectrum.

In present research, a number of chromophores with large two-photon absorption cross sections have been provided by theoretical and experimental studies.<sup>10–14</sup> Among them, symmetrically substituted stilbene-type chromophores (D-B-D) are most widely noticed: first, because of their larger two-photon absorption cross section values ( $\delta_{2\text{PA}}$ ) as compared to the respective asymmetric counterparts,<sup>14</sup> and second because they offer the advantage of high transmission at the range of visible spectrum (400–800 nm). Although symmetric molecules (D-B-D) show very small dipole moments in the ground state, quantum chemical calculations have confirmed that the substantial change in both transition dipole moment and quadrupole moment<sup>11</sup> upon excitation for this type of molecules contributes to inter-molecular charge transfer (ICT) and results in their larger two-photon absorptivities. Therefore, to synthesize this type of symmetric chromophores is of great importance to their applications. As reported synthesis methods of symmetric molecules, Wittig<sup>12</sup> and Heck<sup>13</sup> reactions are considered as the general approaches. However, both of these methods operate complicatedly and require high expenditure. Recently, a series of new symmetrically substituted stilbene chromophores exhibiting great two-photon absorption (2PA) cross section have been synthesized in our research group. The synthesis procedure, the systematic measurements of one-photon/two-photon as well as three-photon absorption cross section, and one-photon/two-photon fluorescence of these new dyes are reported in this paper.

## Experimental

**Synthesis and Characterizations.** IR spectra were measured on a Nicolet FT-IR 5DX spectrometer. Nuclear magnetic resonance spectra were measured on a FX-90Q NMR spectrometer. Element analyses and mass spectra were performed on Perkin 2400 (II) and HP 5989 mass spectra instruments, respectively.

Substituted aminobenzaldehydes, e.g. 4-(*N*-2-hydroxyethyl-*N*-methyl amino)benzaldehyde (1a), 4-pyrrolidinyl benzaldehyde (1b), and 4-(*N,N*-diethylamino)benzaldehyde (1c) were synthesized according to the methods reported.<sup>15</sup> Under the anhydrous and oxygen-free conditions, a mixture of  $\text{TiCl}_4$  (2.2 mL, 20 mmol), zinc (4.4 g, 60 mmol), sodium metal (2.3 g, 100 mmol) and 75 mL of dry tetrahydrofuran (THF) were stirred in the flask at room temperature. After refluxing for one hour, the black mixture was obtained; the contents were then cooled to room temperature. A solution of compound (1a) was injected slowly into the flask and the contents were further refluxed for 20 h. Then they were cooled, hydrolyzed by adding dropwise 5% HCl and neutralized by using 2 M sodium hydroxide solution. The mixture was extracted with chloroform and the organic layer was removed by evaporation. Then this layer was purified by column chromatography on silica gel using an appropriate solvent as eluent. Trans-4,4'-bis[*N*-(2-Hydroxyethyl-*N*-methylamino)stilbene (BHMAS), green-yellow needle crystals with yield of 50% and mp 172.0 °C. MS,  $m/z$  326 ( $\text{M}^+$ ), 295, 249, 132. Element analysis: Calcd for C. H. N: C, 73.59, H, 8.03; N, 8.59%. Found: C, 73.15; H, 8.42; N, 8.91%.  $^1\text{H}$  NMR ( $\text{DMF}-d_6$ )  $\delta$  7.40 (4H, d,  $J = 8.77$  Hz), 6.91 (2H, s), 6.75 (4H, d,  $J = 8.78$  Hz), 3.5–3.7 (8H, m, 4.39), 3.02 (6H, s). IR 3277–3282 (–OH), 3020.2 (aromatic C=C–H, w), 1609.1, 1521.4 (aromatic C=C, s), 965.13  $\text{cm}^{-1}$  (trans-CH=CH, ms).

Using a similar method, we synthesized trans-4,4'-bis(diethylamino)stilbene (BDEAS) with yellow slice crystals with 54% yield. Mass spectrum, MS  $m/z$  322 ( $\text{M}^+$ ), 307, 278, 263, 146. Element analysis: Calcd for C. H. N: C, 81.93; H, 9.37; N, 8.69%. Found: C, 81.45; H, 8.58; N, 8.36%.  $^1\text{H}$  NMR ( $\text{CDCl}_3$ )  $\delta$  7.38 (4H, d,  $J = 8.74$  Hz), 6.86 (2H, s), 6.78 (4H, d,  $J = 8.76$  Hz), 3.82–2.82 (8H, m), 1.18 (12H, t,  $J = 6.54$  Hz). IR 3017.9 (aromatic C=C–H, w), 1608.8, 1523.5 (aromatic C=C, s), 966.75  $\text{cm}^{-1}$  (trans-CH=CH, ms).

The green-yellow crystals, trans-4,4'-di(1-pyrrolidinyl)stilbene (DPS), were obtained with a yield of 65% and mp 298.9 °C. Mass spectrum,  $m/z$  318 ( $\text{M}^+$ ), 289, 275, 262, 159. Element analysis: Calcd for C. H. N: C, 82.97; H, 8.23; N, 8.80%. Found: C, 83.36; H, 7.88; N, 8.45%.  $^1\text{H}$  NMR ( $\text{CDCl}_3$ )  $\delta$  7.21 (4H, d,  $J = 7.64$  Hz), 6.79–6.22 (6H, m), 3.63–2.76 (8H, m), 2.18–1.83 (8H, m, 6.68). IR 3013.5 (aromatic C=C–H, w), 1607.2, 1522.4 (aromatic C=C, s), 961.07  $\text{cm}^{-1}$  (trans-CH=CH, ms).

#### One-Photon Absorption and Multi-Photon Absorption.

Linear absorption spectra with the concentration of  $1.0 \times 10^{-5}$  mol  $\text{dm}^{-3}$  in DMF have been measured from quartz cuvettes of 1 cm path on Hitachi U-3500 recording spectrophotometer. Meanwhile, the linear transmittance spectra were measured at the concentrations of 0.005 mol  $\text{dm}^{-3}$  for BHMAS and BDEAS, and of 0.0005 mol  $\text{dm}^{-3}$  for DPS. The solvents are toluene for DPS and BDEAS, and DMF for BHMAS.

Two-photon induced and three-photon induced absorptivity were measured by direct nonlinear optical transmission (NLT), wherein the transmission ( $T = I/I_0$ ) of a sample was measured as a function of incident intensity  $I_0$ . A mode-locked Nd:YAG laser operating at 1064 nm, pulse duration of 40 ps, angular divergence of 0.4 mrad and pulses repetition of 10 Hz was used as the pump source to pump OPA (Optical Parameter Amplifier) system operating at 10 Hz, tuned between 400–2000 nm. Two Glan prisms were used to change the incident energy, while an  $f = 15$  cm lens was used to focus the incident beam on the chromophore solution. Double-detector energy-meter (EPM 2000, Molelectron) was used in the measurement of input ( $I_0$ )/output ( $I$ ) energy. The influences from the quartz cell and the linear absorption of the solvents have

been subtracted. The concentrations and solvents are the same as for the measurements of linear transmittance spectra. Then, two-photon absorption cross sections ( $\delta_{2\text{PA}}$ ) and three-photon cross sections ( $\delta_{3\text{PA}}$ ) were calculated by the nonlinear transmissivity ( $T = I/I_0$ ) measured for given input intensity and thickness of a sample solution ( $L$ ) by the following relationships (Eqs. 1–4),<sup>16–17</sup>

$$T = \ln(1 + \alpha_2 LI_0)/\alpha_2 LI_0 \quad (1)$$

$$\delta_{2\text{PA}} = h\nu\alpha_2 = 10^3/N_A C_0 \quad (2)$$

$$I = I_0/(1 + 2\alpha_3 LI_0^2)^{1/2} \quad (3)$$

$$\delta_{3\text{PA}} = (h\nu)^2 \alpha_3 \times 10^3/N_A C_0, \quad (4)$$

where  $\alpha_2$  and  $\delta_{2\text{PA}}$  are the 2PA coefficient (unit of  $\text{cm GW}^{-1}$ ) and the 2PA cross section (unit of  $\text{cm}^{-4} \text{ s photon}^{-1}$ ), respectively;  $\alpha_3$  and  $\delta_{3\text{PA}}$  are the 3PA coefficient (unit of  $\text{cm}^3 \text{ GW}^{-2}$ ) and the 3PA cross section (unit of  $\text{cm}^6 \text{ s}^2 \text{ photon}^{-1}$ ), respectively;  $h\nu$  is the energy of the incident photon,  $N_A$  and  $C_0$  are Avogadro's constant and the molar concentration of solute, respectively.

#### One-Photon Fluorescence and Two-Photon Fluorescence.

One-photon induced fluorescence spectra were recorded on a Shimadzu RF5000U fluoro-photometer under the concentration of  $1.0 \times 10^{-5}$  mol  $\text{dm}^{-3}$  in DMF. Two-photon-induced fluorescence spectra were recorded using a streak camera C5680-01 with a 2 ps resolution under a 740 nm laser pulse, obtained by the same conditions as the TPA cross section measurements. All experimental conditions including the concentrations and the solvents were the same as those of the two-photon absorption measurements.

## Results and Discussion

**Synthesis.** The synthetic routes of chromophores are shown in Scheme 1.

Substituted aromatic aldehydes (1a–c) were prepared by phase transfer catalytic (PTC) reaction of secondary amines (such as *N*-2-hydroxyethyl-*N*-methylamine, pyrrolidine, and diethylamine) with 4-fluorobenzaldehyde.<sup>15</sup> Using an efficient Ti-catalyzed reductive coupling methodology, the symmetrically substituted stilbene derivatives (BHMAS, DPS, and BDEAS) were obtained under anhydrous and oxygen-free conditions. Optimum experiments found that only 1.5-fold molar excess of Zn–Na could validly reduce  $\text{Ti}^{4+}$  to the black slurry of  $\text{Ti}^0$ ; otherwise the purple slurry of  $\text{Ti}^{3+}$  was obtained, which failed in the reductive coupling of compounds (1a–c). The synthesis results indicated that the reductive coupling took place on a non-concerted path<sup>18</sup> and the C–O bonds are broken at different times since the IR spectra data have confirmed that the trans-isomer is stable and the cis-isomer was not obtained. It is emphasized that the substituted aromatic aldehyde having hydroxy group can also give  $\text{Ti}^0$ -induced carbonyl reductive coupling, suggesting that reductive couplings can proceed in the presence of active hydrogen such as from an alcohol.

#### One-Photon Absorption and Multi-Photon Absorption.

Linear absorption and linear transmittance spectra of sample solutions are presented in Fig. 1. The solutions are all yellow and the absorption maximum peaks of three dyes appear at ca. 375 nm with a bandwidth of ca. 100 nm (see Table 1 and Fig. 1). The linear transmittance spectra show that these dye solu-

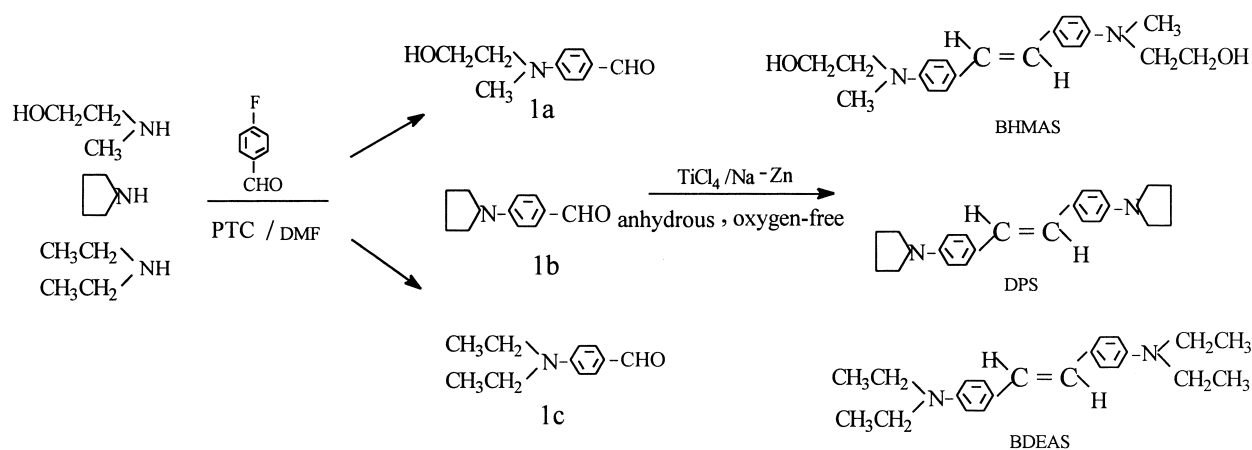


Table 1. Linear and Nonlinear Optical Properties for Three Dyes

Compd.	$\lambda_{\max}^{1PA}/\text{nm}$	$\lambda_{\max}^{2PA}/\text{nm}$ ( $\delta$ , $\text{cm}^4 \cdot \text{s}/\text{photon}$ )	$\lambda_{\max}^{1PF}/(\lambda_{\text{ex}})$ , nm	$\lambda_{\max}^{2PF}/(\lambda_{\text{ex}})$ , nm
BHMAS	374	590 ( $44.5 \times 10^{-48}$ )	406 (367)	437 (740)
DPS	376	602 ( $57.7 \times 10^{-48}$ )	425 (371)	452 (740)
BDEAS	375	730 ( $62.0 \times 10^{-48}$ )	435 (375)	447 (740)

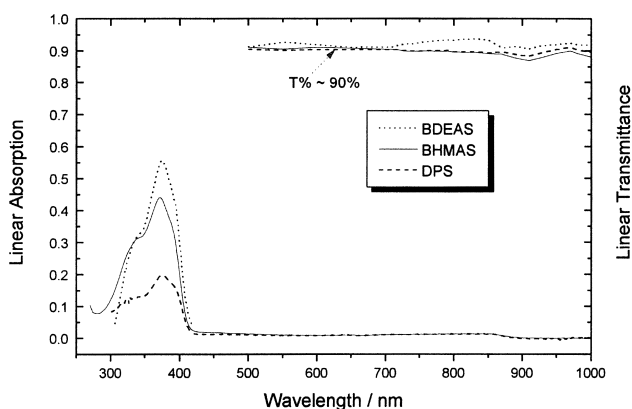
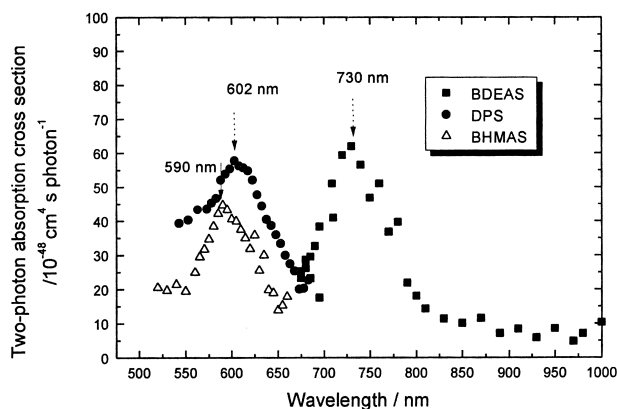
Fig. 1. Linear absorption spectra (in DMF at  $d_0 = 0.00001 \text{ mol dm}^{-3}$ ) and linear transmittance spectra (at  $d_0 = 0.005 - 0.005 \text{ mol dm}^{-3}$ ) of three dyes.

Fig. 2. Two-photon absorption spectra of three dye solutions at 0.005 M for BHMAS and BDEAS, at 0.0005 M for DPS.

tions exhibit the linear transparency of ca. 90% at wavelength  $\geq 500 \text{ nm}$  (see Fig. 1). So the two-photon energy of visible spectrum radiation falls just within the strong linear absorption band around 375 nm.

From Table 1 and Fig. 2, we can see that the TPA cross sections are  $44.5 \times 10^{-48} \text{ cm}^4 \text{ s photon}^{-1}$  for BHMAS,  $57.7 \times 10^{-48} \text{ cm}^4 \text{ s photon}^{-1}$  for DPS, and  $62.0 \times 10^{-48} \text{ cm}^4 \text{ s photon}^{-1}$  for BDEAS. These  $\delta_{2PA}$  values are much higher than those for commonly used commercial dyes such as Rhodamine and corresponding asymmetric substituted stilbene derivatives.<sup>14,19</sup> We can also observe that the 2PA maximum peaks are nearly twice as high as those of the 1PA maximum peaks for the respective dye. The peaks of the one-photon absorption

of three new dyes, as discussed above, are all at the same position ( $\approx 375 \text{ nm}$ ), while the maximum 2PA peak is at 730 nm for BDEAS, and at 602 nm for DPS, and at 590 nm for BHMAS. Clearly, BDEAS exhibits a significant shift of the position of the two-photon resonance to longer wavelength. Such a bathochromic shift of the two-photon absorptivity for BDEAS suggests that it possesses the stabilization of the two-photon state, which has contributed to the two-photon absorption cross section. The theoretical explanation for the fact that the red-shift of TPA spectrum can enhance TPA cross section is the following.

The molecular TPA cross section,  $\delta_{\text{TPA}}$ , is proportional to the imaginary part of the third-order polarizability ( $\gamma$ ),<sup>11</sup> and it can

be expressed as Eq. 5 if the frequency ( $\omega$ ) is neglected,<sup>20–21</sup>

$$\delta_{\text{TPA}} \propto \gamma_{\text{xxxx}} = 24 \frac{M_{\text{ge}}^2}{E_{\text{ge}}^2} \left[ \frac{\Delta\mu_{\text{ge}}^2}{E_{\text{ge}}^2} - \frac{M_{\text{ge}}^2}{E_{\text{ge}}} + \sum_e \frac{M_{\text{ee}'}^2}{E_{\text{ge}'}} \right], \quad (5)$$

where  $\Delta\mu_{\text{ge}}$  is the difference of dipole moment between the ground state ( $S_0$ ) and the first excited state ( $S_1$ );  $M_{\text{ge}}$  or  $M_{\text{ee}'}$  is the transition dipole moment between  $S_0$  and  $S_1$  or between  $S_1$  and the second excited state ( $S_2$ ).  $E_{\text{ge}}$  or  $E_{\text{ge}'}$  is the transition energy from  $S_0$  to  $S_1$  or from  $S_0$  to  $S_2$ . We have calculated some of the parameters mentioned above using ZINDO program with a view to the three-level model; these are presented in Table 2. It can be seen that, for three samples, the influences of first two terms in Eq. 5 upon their TPA cross section are equal since all the parameters related to the  $S_1$  (lowest one-photon allowed excited state) are the same; for example, the values of  $\Delta\mu_{\text{ge}}$ ,  $M_{\text{ge}}$ , and  $E_{\text{ge}}$  for three samples are ca. 0.03 D, ca. 9.3 D, and ca. 3.31 eV, respectively (see Table 2). But the parameters such as  $E_{\text{ge}'}$ ,  $M_{\text{ee}'}$  related to the  $S_2$  state are different; for example, the  $\lambda_{\text{max}}^{2\text{PA}}$  is 2.10 eV for BHMAS, 2.07 eV for DPS, and 1.70 eV for BDEAS, respectively. Small  $\lambda_{\text{max}}^{2\text{PA}}$  (eV) value for BHMAS means it may have small  $E_{\text{ge}'}$  value since two-photon absorption process refers to a molecule simultaneous absorption of two photon on the excitation from the ground state to the excited state, i.e.  $E_{\text{ge}'} = 2h\nu$ . Clearly, the small  $E_{\text{ge}'}$  value for BDEAS shows its red-shift in 2PA spectrum, which makes a positive contribution to two-photon absorptivity, as shown in Eq. 5. The origin of this two-photon state stabilization may be substantial intra-molecular charge transfer (ICT) upon excitation of  $S_0 \rightarrow S_2$ , characterized by the

transition dipole moments ( $M_{\text{ee}'}$ ).<sup>11</sup> From Table 2, it can be also seen that the value of  $M_{\text{ee}'}$  is 13.0 D for BHMAS, 13.6 D for DPS, and 14.4 D for BDEAS, that is, and increase of the transition dipole moment corresponds to a red-shift of TPA spectrum.

In addition, we have also observed (shown in Fig. 3) that DPS exhibited obvious three-photon absorption behavior. The three photon absorption coefficient ( $\alpha_3$ ) and cross section ( $\delta_{3\text{PA}}$ ) values are  $20.4 \times 10^{-20} \text{ cm}^3 \text{ W}^{-2}$  and  $27.3 \times 10^{-76} \text{ cm}^6 \text{ s}^2$ , respectively under ca. 990 nm laser irradiation, which are almost triple the values for the peak of one-photon absorption.

**One-Photon Fluorescence and Two-Photon Fluorescence.** All the sample solution emit strong blue fluorescence, easily observed by the naked eye although the solutions are yellow. For a comparative study, one-photon fluorescence (1PF) and two-photon fluorescence (2PF), as well as linear absorption spectra are plotted together. From Figs. 4–6 and Table 1, we can see that the maximum peaks of the 1PF are at  $\lambda_{\text{max}}^{1\text{PF}} = 406 \text{ nm}$  with a bandwidth of 50 nm for BHMAS, at  $\lambda_{\text{max}}^{1\text{PF}} = 425 \text{ nm}$  with a bandwidth of 54 nm for DPS, and at  $\lambda_{\text{max}}^{1\text{PF}} = 435 \text{ nm}$  with a bandwidth of 60 nm for BDEAS.

When pumped by 740 nm laser irradiation, strong two-photon induced upconversion blue fluorescence can be observed, with the maximum peaks at  $\lambda_{\text{max}}^{2\text{PF}} = 437 \text{ nm}$  and a bandwidth of 36 nm for BHMAS,  $\lambda_{\text{max}}^{2\text{PF}} = 452 \text{ nm}$  and a bandwidth of 30 nm for DPS, and  $\lambda_{\text{max}}^{2\text{PF}} = 447 \text{ nm}$  and a bandwidth of 36 nm for BDEAS. Obviously, there is a red-shift for two-photon fluorescence in comparison with one-photon fluorescence. We propose that the re-absorption effect<sup>22</sup> is responsible for this red-shift behavior of chromophores. As shown in Figs. 4, 5, and 6, there is a partial overlap from 370 to 430 between the

Table 2. The ZINDO Program Calculated Parameters Using the Three-Level Model

Compd.	$M_{\text{ge}}$ /Debye	$\Delta\mu_{\text{ge}}$ /Debye	$E_{\text{ge}}$ /nm <sup>a)</sup>	$M_{\text{ee}'}$ /Debye	$\lambda_{\text{max}}^{2\text{PA}}$ /nm <sup>a)</sup>
BHMAS	9.3	0.03	374 (3.32 eV)	13.0	590 (2.10 eV)
DPS	9.3	0.02	376 (3.30 eV)	13.6	602 (2.07 eV)
BDEAS	9.4	0.04	375 (3.31 eV)	14.4	730 (1.70 eV)

a) experimental data.

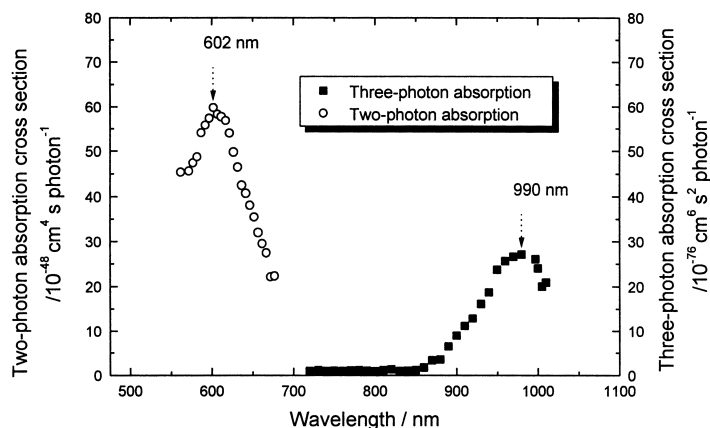


Fig. 3. Multi-photon absorption spectra of DPS in toluene at  $d_0 = 0.0005 \text{ M}$ .

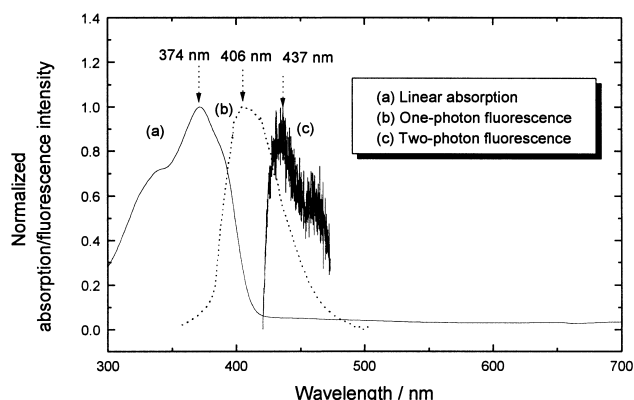


Fig. 4. Linear absorption, one-photon fluorescence and two-photon fluorescence spectra of BHMAS solution.

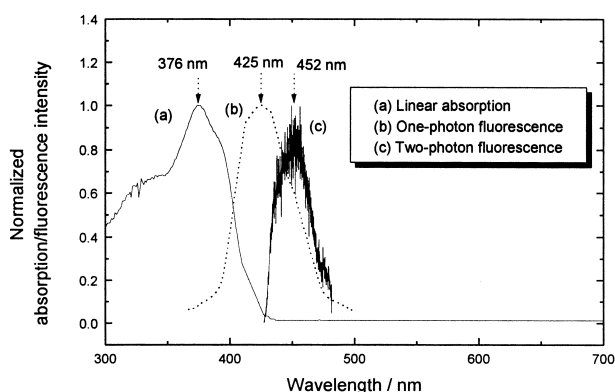


Fig. 5. Linear absorption, one-photon fluorescence and two-photon fluorescence spectra of DPS solution.

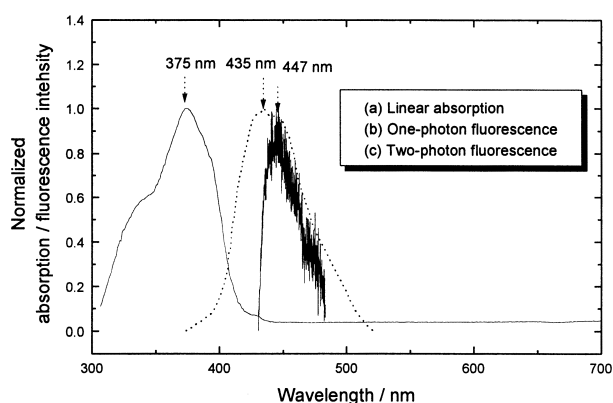


Fig. 6. Linear absorption, one-photon fluorescence and two-photon fluorescence spectra of BDEAS solution.

blue side of the one-photon induced fluorescence band (b) and the red side of the linear absorption (a). The one-photon induced fluorescence spectra were measured at a very low concentration of  $0.00001 \text{ mol dm}^{-3}$ ; thus the re-absorption effect of the 1PF spectra can be neglected. In the case of two-photon excitation, we have to use a relatively concentrated solution ( $0.005\text{--}0.0005 \text{ mol dm}^{-3}$ ) in order to obtain stronger fluorescence. Since the 740 nm laser beam can pass through the whole solution length without depletion, the fluorescence

emission is not only from the surface layer, but also from within the solution sample. The re-absorption of the shorter wavelength fluorescence by the concentrated sample within the 1 cm propagation length can no longer be neglected. The intensity of short-wavelength side of two-photon induced fluorescence spectra reduced greatly. So the short-wavelength side became steeper and the central wavelength red-shifted.

### Conclusions

Three new symmetrically substituted silbene derivatives (BHMAS, DPS, and BDEAS) have been synthesized by reductive coupling using effective  $\text{Ti}^{0}$ -valent reagent, accessible from  $\text{TiCl}_4$  by reduction with Na–Zn couple, and their chemical structures have been characterized by IR,  $^1\text{H}$  NMR, MS and elemental analyses, respectively. These dye solutions exhibit large two-photon absorption cross section, resulting in strong two-photon-induced blue fluorescence. The experiments and ZINDO calculations have shown that the parameters such as  $E_{\text{ge}}$ ,  $M_{\text{ge}}$ , and  $\Delta\mu_{\text{ge}}$ , related to the first excited state are the same, but the parameters such as  $\lambda_{\text{max}}^{2\text{PA}}$ ,  $M_{\text{ee}}$  related to the second excited state are different. A bathochromic shift of 2PA spectrum accompanies an increase in TPA cross section due to the stabilization of the second excited state.

This work was supported by the grant for State Key Program of China.

### References

- 1 M. Göpper-Mayer, *Ann. Phys., (Leipzig)*, **9**, 273 (1931).
- 2 W. L. Peticolas, *Ann. Rev. Phys. Chem.*, **18**, 233 (1967).
- 3 W. Denk, J. H. Strickler, and W. W. Webb, *Science*, **248**, 73 (1990).
- 4 J. D. Bhawalkar, G. S. He, and P. N. Prasad, *Rep. Prog. Phys.*, **59**, 1041 (1996).
- 5 A. Simeonov, M. Matsushita, E. A. Juban, E.-H. Z. Elizabeth, T. Z. Hoffman, A. E. Beuscher, M. J. Taylor, P. Wirsching, W. Rettig, J. K. McCusker, R. C. Stevens, D. P. Millar, P. G. Schultz, R. A. Lerner, and K. D. Janda, *Science*, **290**, 307 (2000).
- 6 B. H. Cumpston, S. P. Ananthavel, S. Barlow, D. L. Dyer, J. E. Ehrlich, L. L. Erskine, A. A. Heikal, S. M. Kuebler, I.-Y. Sandy Lee, D. M. Maughon, J. Q. Qin, H. Rockel, M. Rumi, X. L. Wu, S. R. Marder, and J. W. Perry, *Nature*, **398**, 51 (1999).
- 7 C. L. Caylor, I. Dobrianov, C. Kimme, R. E. Thorne, W. Zipfel, and W. W. Webb, *Phys. Rev. E.*, **59**(4), R3831 (1999).
- 8 J. D. Bhawalkar, S. J. Pan, A. Shih, J. K. Samarbandu, J. Swiatkiewicz, B. A. Reinhardt, P. N. Prasad, and P. C. Cheng, *Polym. Commun.*, **38**, 4551 (1997).
- 9 K. D. Belfield, D. J. Hagan, E. W. V. Stryland, K. J. Schafer, and R. A. Negres, *Organic Lett.*, **1**, 1575 (1999).
- 10 O.-K. Kim, K.-S. Lee, H. Y. Woo, K.-S. Kim, G. S. He, J. Swiatkiewicz, and P. N. Prasad, *Chem. Mater.*, **12**, 284 (2000).
- 11 M. A. Albota, D. Beljonne, J. L. Bredas, J. E. Ehrlich, J. Y. Fu, A. A. Heikal, S. E. Hess, T. Kogej, M. D. Levin, S. R. Mader, D. M. Maughon, J. W. Perry, H. Rocket, M. Rumi, G. Subramanian, W. W. Webb, X.-L. Wu, and C. Xu, *Science*, **281**, 1653 (1998).
- 12 M. Rumi, J. E. Ehrlich, A. A. Heikal, J. W. Perry, S. Barlow, Z. Hu, D. M. Maughon, T. C. Parker, H. Rockel, S. Thayumanavan, S. R. Marder, D. Beljonne, and J.-L. Bredas, *J.*

*Am. Chem. Soc.*, **122**, 9500 (2000).

13 B. A. Reinhard, L. L. Brott, S. J. Clarson, A. G. Dillard, J. C. Bhatt, R. Kannan, L. Yuan, G. S. He, and P. N. Prasad, *Chem. Mater.*, **10**, 1863 (1998).

14 X.-M. Wang, C. Wang, W.-T. Yu, Y.-F. Zhou, X. Zhao, Q. Fang, and M. H. Jiang, *J. Can. Chem.*, **79**, 174 (2001).

15 X.-M. Wang, Y.-F. Zhou, W.-T. Yu, C. Wang, Q. Fang, M.-H. Jiang, *J. Mater. Chem.*, **10**, 2698 (2000).

16 G. S. He, R. Gvishi, P. N. Prasad, and B. A. Reinhardt, *Opt. Commun.*, **117**, 133 (1995).

17 G. S. He, J. D. Bhawalkar, P. N. Paras, and B. A. Reinhardt, *Opt. Lett.*, **20**, 1525 (1995).

18 J. E. McMurry, M. P. Fleming, and K. L. Kees, *J. Org. Chem.*, **43**, 3255 (1978).

19 G. S. He, L. Yuan, N. Cheng, J. D. Bhawalkar, P. N. Prasad, L. L. Brott, S. J. Clarson, and B. A. Reinhardt, *J. Opt. Soc. Am. B.*, **14**, 1079 (1997).

20 F. Meyers, S. R. Marder, B. M. Pierce, and J. L. Bredas, *J. Am. Chem. Soc.*, **116**, 10703 (1994).

21 T. Kogej, D. Beljonne, F. Meyyars, J. W. Perry, S. R. Marder, and J. L. Brédas, *Chem., Phys. Lett.*, **298**, 1 (1998).

22 G. S. He, L. Yuan, Y. Cui, M. Li, and P. N. Prasad, *J. Appl. Phys.*, **81**, 2529 (1997).

---